Electrostatic interaction between two charged dielectric spheres in contact

James Q. Feng
Wilson Center for Research and Technology, Xerox Corporation, 800 Phillips Road, Webster, New York 14580
(Received 29 February 2000)

Of fundamental importance in numerous industrial and natural processes, the problem of two electrified spheres has been studied by many authors. However, the problem of particular importance for understanding electrostatic effects on powder or granular behavior, such as two dielectric spheres both carrying arbitrary amounts of charge, is still open for investigation. In the present work, two touching dielectric spheres of equal size and permittivity but arbitrary amounts of charge are studied by computational means of the Galerkin finite-element method. The effects of permittivity and the ratio of charge on the spheres are the main focus here. Because of the electric polarization, the electrostatic force can become attractive even when the two spheres carry charges of the same sign, due to positive dielectric effects, or to become repulsive for spheres with charges of the opposite sign, due to negative dielectric effects. In the presence of dielectrophoretic effect, whether the electrostatic force between the two spheres is attractive or repulsive is found to be determined by the ratio of charge on the two spheres.

PACS number(s): 41.20.Cv, 02.70.Dh

I. INTRODUCTION

Understanding the electrostatic interaction between two charged dielectric spheres in contact is desired for scientific description of the behavior of powder or granular materials that consist of electrically insulating particles [1]. Those insulating (or dielectric) particles naturally acquire charge through the mechanism of triboelectricity by contacting each other or the container walls [2]. The amount of charge on each particle and the distribution of charge among the particles are expected to influence the rheological behavior of powder or granular materials, which determines the degree of difficulty in accomplishing well controlled material transportation as needed in many technological applications. For example, the toner used in electrophotographic copiers and printers is typically a cohesive powder, with insulating particles of a diameter about 10 μm consisting of a pigment dispersed in a polymer resin. These toner particles are designed to acquire charge through the mechanism of triboelectricity ([3–5]). In electrophotographic processes, the toner must be delivered from a toner reservoir to the image development zone. Stringent requirements of accurate control of toner transportation in modern electrophotographic color printing engines call for a fundamental understanding of the electrostatic effects on charged particle interactions in a dielectric powder.

To enable detailed analysis, the problem needs to be simplified by reducing the number of interacting particles. A relevant model should involve at least two spheres. Considering two touching spheres is desired, because particles in powder or granular materials will make contact with each other. Powder with a narrow particle size distribution can be manufactured. But the charge distribution among dielectric particles is unlikely to become arbitrarily narrow due to the stochastic nature of the triboelectric process. If the effect of particle size distribution is ignored, considering two equal-sized dielectric spheres allows attention to be focused on the effect of charge distribution among particles and the effect of permittivity of the dielectric particle materials.

Of fundamental importance in numerous industrial and natural processes, the problem of two electrified spheres has been studied by many authors including Poisson [6], Lord Kevin [7], Maxwell [8], Russell [9], and others. Most earlier authors considered conducting spheres because of the relatively simpler treatments in boundary conditions. The complete solution in bispherical coordinates (Morse and Feshbach [10]) for two charged conducting spheres in an arbitrarily oriented uniform electric field was obtained by Davis [11]. A less general problem of two equal-sized, uncharged conducting spheres in a uniform electric field at a fixed orientation was also solved in bispherical coordinates by Levine and McQuarrie [12] for calculating the dielectric constant of simple gases. The investigation of two uncharged dielectric spheres in a uniform electric field in bispherical coordinates starts with the work of Goyette and Navon [13], who restricted the treatment to equal-sized spheres in an electric field of a fixed orientation. The problem was further generalized through the efforts of Love [14], Stoy [15,16], and Chaumet and Dufour [17]. To understand the atmospheric phenomenon of removing aerosol particles by hydrometeor scavenging, the electrostatic force between a conducting sphere and a dielectric sphere was calculated by Hall and Beard [18] and Grover [19] in bispherical coordinates.

The problem involving two charged dielectric spheres was not addressed in the literature until a recent publication by Nakajima and Sato [20]. However, these authors mainly focused on expounding the mathematical derivations, showing limited results for applicability demonstration of their reexpansion method in different problem configurations. For instance, the exemplifying cases presented by Nakajima and Sato [20] include two conducting spheres, a charged dielectric sphere near a grounded conducting plane, a charged dielectric sphere on a thick plane wall (approximated as a very large dielectric sphere) without surface charge, and an uncharged dielectric sphere on a thick plane wall with surface charge. The problem of particular relevance to the electrostatic effects on powder or granular behavior, such as two dielectric spheres each carrying an arbitrary amount of charge, is still heretofore open for investigation.

In the two-sphere system with finite separation, material

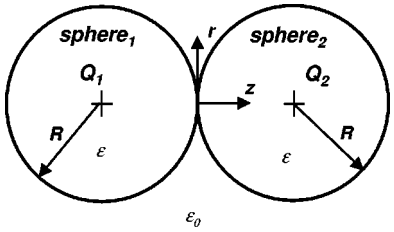

FIG. 1. Definition sketch of two touching dielectric spheres of equal size.

interfaces fit coordinate surfaces in a bispherical coordinate system, so that solutions to the Laplace equation can be obtained by separation of variables [10]. Hence, most authors (e.g., [11–19]) were tempted to derive formulas in bispherical coordinates. Elegant as the bispherical coordinate solutions may seem to be, practical calculations can rarely be done without implementation of a computer code for carrying out numerical computations due to the fact that a large number of terms in an infinite series needs to be evaluated, especially when the gap between the two spheres diminishes. Moreover, the bispherical coordinate system cannot be applied in the strict sense to cases when the spheres touch because of mathematical singularities. This fact led O'Meara and Saville [21] to seek other means of studying two touching spherical conductors in an electric field.

When the particles are of spherical shape, multipole expansion in terms of Legendre polynomials (cf. [22–24]) or in terms of image charge series (cf. [7,25–27]) can be used to determine the electric potential distribution. Over the years, the multipole expansion method has been used in considering a charged dielectric sphere touching a plane surface, as an extreme configuration of the two-sphere system, for calculating the electrostatic adhesion force on electrophotographic toner particles [28–31]. Here again, numerical computations must be carried out because large numbers of multipole terms are needed to obtain a converged representation of the actual electric field that accurately satisfies all the boundary conditions.

In the present work, a numerical technique based on the well-established Galerkin finite-element method [32] is employed; therefore, the intrinsic limitations to two spheres (as in the bispherical coordinate system) and the restriction on material interface shapes (as in multipole expansions) are eliminated. Sophisticated mathematical derivations become unnecessary in computing finite-element solutions. Moreover, the finite-element method is readily applicable to much more complicated problem configurations if future extension of the present analysis is desired. For simplicity, two touching dielectric spheres of equal size and permittivity are examined with each sphere carrying an arbitrary amount of charge. The effects of particle permittivity (or dielectric constant) and the ratio of charge on the two spheres are the main focus here.

II. PROBLEM FORMULATION

As shown in Fig. 1, the problem considered here consists of two touching dielectric spheres, namely, sphere 1 and sphere 2, of the same radius R and the same permittivity ϵ, carrying charges Q_1 and Q_2 in a dielectric surrounding medium of permittivity ϵ_0. For simplicity, the charge on each sphere is assumed to be distributed uniformly over the surface. For convenience, variables are made dimensionless by measuring length in units of R, electric potential in units of $Q_2/(4\pi\epsilon_0 R)$, total charge on sphere in units of Q_2, and surface charge density in units of $Q_2/(4\pi R^2)$. Thus, sphere 1 has a net charge $Q=Q_1/Q_2$, whereas the net charge on sphere 2 becomes unity. The dimensionless net charge on the spheres becomes the same as their dimensionless surface charge densities. In the absence of an externally applied electric field, the problem becomes axisymmetric about the line connecting the centers of the two spheres, i.e., the z axis of the zr axisymmetric cylindrical coordinates used in the present work.

The electric potential V, inside and outside the spheres, is governed by the Laplace equation

$$\nabla^2 V=0. \tag{1}$$

At dielectric material interfaces such as the surfaces of the spheres, the continuity of the tangential component of electric field and surface charge induced change in the normal component of the electric displacement vector are described by

$$V_i=V_o, \quad \mathbf{n}\cdot(\kappa\nabla V_i-\nabla V_o)=\begin{cases} Q, & \text{on } S_1 \\ 1, & \text{on } S_2, \end{cases} \tag{2}$$

where $\kappa\equiv\epsilon/\epsilon_0$ is the dielectric constant with respect to the permittivity of the surrounding medium ϵ_0. The subscripts i and o in the present work are used to denote variables associated with regions inside and outside the spheres. The same variables without those subscripts apply in all the regions.

Along the axis of symmetry, the Neumann boundary condition is applied as

$$\mathbf{n}\cdot\nabla V=0, \quad \text{on } S_{\text{sym}}. \tag{3}$$

At a large distance on the asymptotic boundary, a consideration of the monopole charge alone should be sufficiently accurate, the asymptotic boundary condition is applied in a Dirichlet form as

$$V=\frac{Q}{\sqrt{(z+1)^2+r^2}}+\frac{1}{\sqrt{(z-1)^2+r^2}}, \quad \text{on } S_{\text{asymp}}. \tag{4}$$

The electrostatic interaction force acting on sphere 1 (denoted as F), which should only have a nonzero z component, can be computed by integrating the difference of the Maxwell stress tensor across the material interface over the surface of sphere 1 as

$$F=\frac{1}{\pi}\int_{S_1}\left\{\frac{n_z}{2}\left[\left(1-\frac{1}{\kappa}\right)(\mathbf{n}\cdot\nabla V_o)^2+(\kappa-1)(\mathbf{t}\cdot\nabla V_o)^2 - \frac{2Q}{\kappa}(\mathbf{n}\cdot\nabla V_o)-\frac{Q^2}{\kappa}\right]-t_z Q(\mathbf{t}\cdot\nabla V_o)\right\}dS, \tag{5}$$

where n and t denote the local unit normal and unit tangential vectors on the surface, and F is a dimensionless quantity scaled in units of $Q_2^2/(16\pi\epsilon_0 R^2)$. In the absence of an ex-

ternally applied electric field, the total electrostatic force acting on sphere 2 is simply given by $-F$.

Now, the problem can be treated by solving the electric potential distribution for a given value of Q and then determining F from V_o and Q according to Eq. (5). This approach requires tedious solution of V_o for many different values of Q to gain adequate insights into the general behavior of F as a function of Q for a given particle permittivity.

From a phyical point of view, however, the electrostatic force can be expressed as a sum of three lumped terms

$$F(Q)=\alpha Q^2-\beta Q+\gamma, \tag{6}$$

as similarly discussed for the case of electric field detachment of a charged dielectric sphere from a plane surface (cf. [24,29,33]). On the right side of Eq. (6), the first term is due to the attraction from the image charge of Q induced in sphere 2. The second term represents the Coulomb force from the interaction between Q and the electric field generated by the charge on sphere 2. The third term describes the fact that a net dielectrophoretic force can be induced by the electric field from the charge on sphere 2 (which is a constant normalized as unity in the present notation) even when sphere 1 does not carry net charge (i.e., $Q=0$). In general, the coefficients α, β, and γ can be functions of the particle permittivity and geometric configuration such as the particle size ratio as well as the distance between particles. For the present problem, because of symmetry in the two equal-sized spheres with the same value of permittivity, a relationship

$$\gamma=\alpha \tag{7}$$

is expected. Thus, only two independent points on the parabola, as described by Eq. (6), are required to determine the two unknown coefficients α and β for a complete description of the behavior of $F(Q)$ for a given value of particle permittivity κ.

III. COMPUTATIONAL TECHNIQUES

Instead of specifically formulating the problem in bispherical coordinates or going through a multipole expansion procedure for spherical geometry, the computational technique used in the present work is based on a straightforward application of the well-established Galerkin finite-element method that is generally applicable to virtually any geometric configuration and equation system [32]. Therefore, the two-dimensional problem domain (in zr space) is divided into a set of nine-node quadrilateral elements (see Fig. 2), with the elements at the point where two spheres touch becoming triangular shaped as degenerated from the quadrilateral elements by collapsing one of the element sides to acommodate the cusp geometry. These degenerated elements need no special treatment in code implementation, in view of previous experience with similar circumstances [33–35] and the comments of Hughes [36]. With the convenience of the finite-element domain discretization, the mesh is made much finer near the surfaces of the spheres as needed for accurate evaluation of the expected more significant variations of electric potential than elsewhere.

On each element, which is mapped onto a unit square in the $\xi\eta$ (computational) domain, the unknown electric potential is expressed in an expansion of nine biquadratic finite-element basis functions, each associated with an element node. As a consequence, the nodal values of electric potential become the expansion coefficients. By the same token, the spatial coordinates are expressed in an expansion of the same type of basis functions with the nodal coordinates as the expansion coefficients, which are commonly referred to as isoparametric mapping. Galerkin's method of weighted residuals is applied by multiplying the Laplace equation (1) with each finite-element basis function as used for the expansion of electric potential and integrating the weighted equation over the entire problem domain [37]. The obtained weighted residual equations is a set of algebraic equations with finite degrees of freedom.

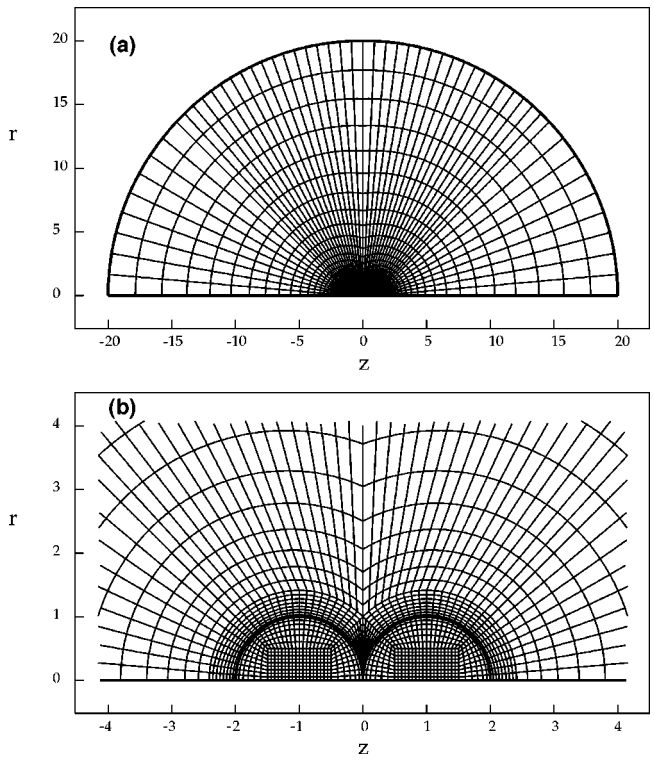

FIG. 2. Finite-element mesh for two touching spheres: (a) general view; (b) detail around touching spheres.

The unknown electric potential here can be determined by solving a set of linear residual equations, which takes only one step of Newton iterations as usually used for solving nonlinear algebraic equations (e.g., [37,38]). Once the electric potential distribution is obtained, the electrostatic interaction force on each sphere can be computed according to Eq. (5), in ''post-processing'' the solution. In the present work, the integral is discretized and computed in the same way as with the finite-element method in computing weighted residual equations. Actually, Eq. (5) is added into the set of weighted residual equations from Laplace's equation as an auxiliary equation associated with an auxiliary unknown F. Thus, F is solved simultaneously with the electric potential V.

To reduce errors arising from induced multipoles in using Eq. (4), the asymptotic boundary is positioned at a large spherical surface of radius 20 centered at the coordinate origin where the two spheres touch. Thus, the distance from each sphere to the asymptotic boundary is much greater than

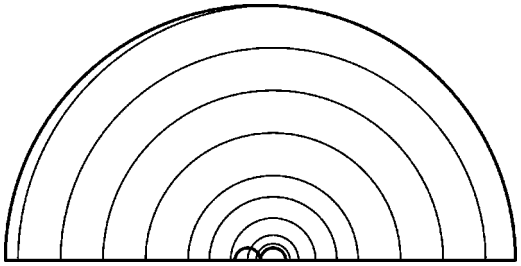

FIG. 3. Equipotential contours of the case with $\kappa=1$ and $Q=0$. The equipotential values are 0.05, 0.06, 0.075, 0.1, 0.15, 0.2, 0.3, 0.5, 0.75, and 1.

10, where the effects of higher-order multipoles than that of the monopole become negligible.

IV. RESULTS AND DISCUSSION

Because the problem is solved here by means of numerical computations, the accuracy of the numerical results needs be examined first. An effective indicator is found to be the difference between the directly computed values of $|F|$ on sphere 1 and the magnitude of force on sphere 2, which can be appreciated when considering a simple case with $\kappa=1$ and $Q=0$. It is immediately recognized from Eq. (5) that $F=0$ on sphere 1 for $\kappa=1$ and $Q=0$ because each term on the right side is multiplied by a factor of 0. However, in computing the force on sphere 2 by integrating the Maxwell stress tensor over S_2, Q in Eq. (5) should be replaced by 1. Thus, the value of force so computed cannot be exactly zero and it represents the magnitude of the actual numerical error. As expected, the value of force on sphere 2 at $\kappa=1$ and $Q=0$ varies with the number of elements used in tessellation of the problem domain. For the mesh shown in Fig. 2 with 2250 elements used in the domain tessellation, the directly computed value of force on sphere 2 at $\kappa=1$ and $Q=0$ is 8.26×10^{-5}, indicating that the numerical error can be considered negligible here. Figure 3 shows the equipotentials of electric field for $\kappa=1$ and $Q=0$, where the equipotential surfaces are concentric spherical surfaces around sphere 2 without any modification due to the presence of sphere 1, as physically expected. For comparison, the equipotentials of electric field for $\kappa=3$ and $Q=0$ are illustrated in Fig. 4 where equipotential surfaces are distorted and electric field strength is reduced in sphere 1.

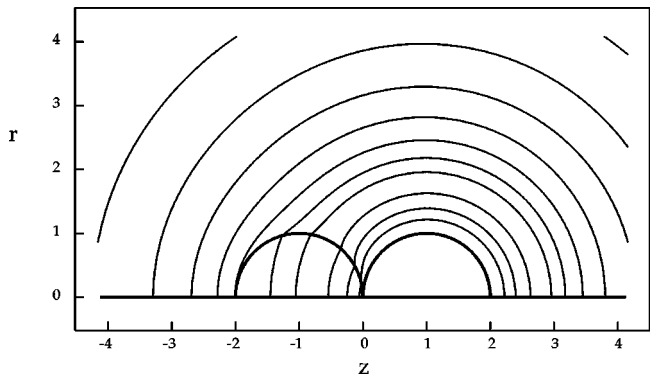

FIG. 4. Equipotential contours of the case with $\kappa=3$ and $Q=0$. The equipotential values are 0.1, 0.15, 0.2, 0.25, 0.3, 0.35, 0.4, 0.45, 0.5, 0.6, 0.7, and 0.8.

The case with $\kappa=1$ is special because the effects of induced multipoles in dielectric media are completely eliminated. Without the polarization effects, α in Eq. (6) becomes zero and the parabola in $Q-F$ space is degenerated into a straight line through the origin $Q=F=0$. The slope of the line $-\beta$ can be obtained by computing F at $Q=1$. From physical consideration, F should become -1 at $Q=1$, reflecting a mutually repulsive force between two spheres carrying the same amount of charge. Here, the computed values of F on sphere 1 and force on sphere 2 are $-1.000\,046\,0$ and $1.000\,045\,5$, respectively. Both the deviation from the exact theoretical value and the difference between $|F|$ on sphere 1 and the magnitude of force on sphere 2 are very small here, validating the adequacy of the present finite-element tessellation.

To determine the two unknown coefficients α and β for a complete description of F as a function of Q, in general, the computed values of $F(Q)$ at $Q=0$ and 1 appear to be the most convenient choices. According to Eqs. (6) and (7), α and β can be readily determined from the computed $F(0)$ and $F(1)$ as

$$\alpha=F(0) \quad \text{and} \quad \beta=2F(0)-F(1). \tag{8}$$

As expected, the parabola of $F(Q)$ has two roots at $F=0$ as given by

$$Q=\frac{1}{2}\left[\frac{\beta}{\alpha}\pm\sqrt{\left(\frac{\beta}{\alpha}\right)^2-4}\right]. \tag{9}$$

Noteworthy here is that the two roots are of the same sign and reciprocal to each other as evidenced by

$$\frac{1}{4}\left[\frac{\beta}{\alpha}+\sqrt{\left(\frac{\beta}{\alpha}\right)^2-4}\right]\left[\frac{\beta}{\alpha}-\sqrt{\left(\frac{\beta}{\alpha}\right)^2-4}\right]=1 \tag{10}$$

and the symmetry of the system. Furthermore, in delineating the intervals of Q for attractive and repulsive electrostatic forces, these two roots can serve as the discriminating points.

For the case of dielectric spheres with $\kappa=3$, as representive for the situation of electrophotographic toner particles in air, the computed values of $F(Q)$ at $Q=0$ and 1 are $0.208\,36$ and $-0.774\,82$, respectively. Thus, we have $\alpha=0.208\,36$ and $\beta=1.191\,54$ from Eq. (8). The two roots at $F=0$ are $0.180\,57$ and $5.538\,09$. Because both α and β are positive, F has a minimum value (corresponding to maximum repulsion between the two spheres) at the middle of the interval between the two roots, i.e., $Q_m=\beta/(2\alpha)$ ($=2.859\,33$ for $\kappa=3$). The distribution of electric field for maximum repulsion to occur is shown in Fig. 5 with equipotential contours. The field strength in sphere 1 appears to be much weaker than that in sphere 2, because sphere 1 has greater amount of charge on its surface. Interestingly, the maximum repulsion between the two spheres does not happen when the two spheres carry the same amount of charge (i.e., $Q=1$) as one would have intuitively expected. Also somewhat counterintuitive is that two particles carrying charges of the same sign do not necessarily repel each other, provided the difference between the particle charges is large enough; this is due to the dominant dielectric force.

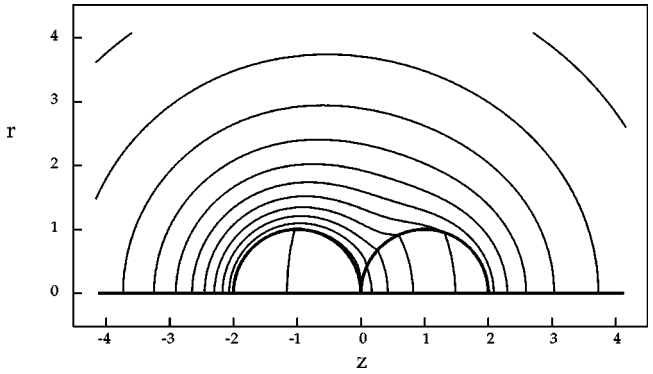

FIG. 5. Equipotential contours of the case with $\kappa=3$ and $Q=2.859\,33$. The equipotential values are in increments of 0.25 from 0.75 to 3.25.

The computational results of α and β are shown as functions of κ in Figs. 6 and 7, respectively. As can be seen, α takes positive values that increases with κ for $\kappa>1$. Positive α represents a positive dielectrophoretic force on sphere 1 in the direction of the gradient of electric field generated by the charge on sphere 2. If $\kappa<1$, α becomes negative corresponding to a negative dielectrophoretic effect that arises when the particles are less polarizable than the surrounding medium. In contrast, β is always greater than 1 except for $\kappa=1$ where β exactly equals 1. Thus, the Coulomb force term in Eq. (6) is always enhanced by the polarization effect.

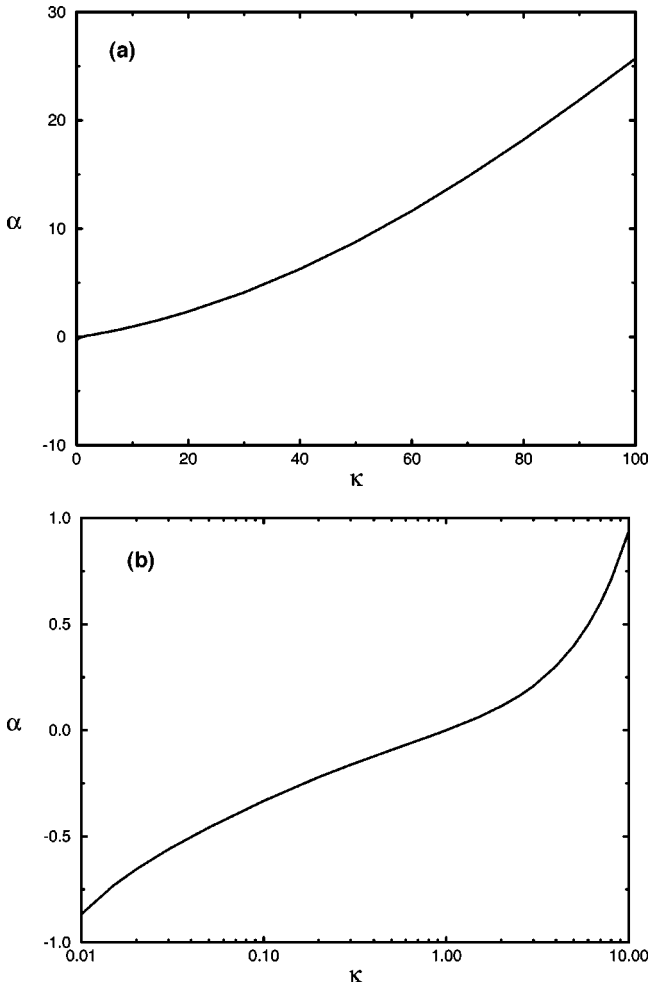

FIG. 6. Plot of α as a function of κ: (a) general view; (b) detail for $\kappa\leqslant 10$.

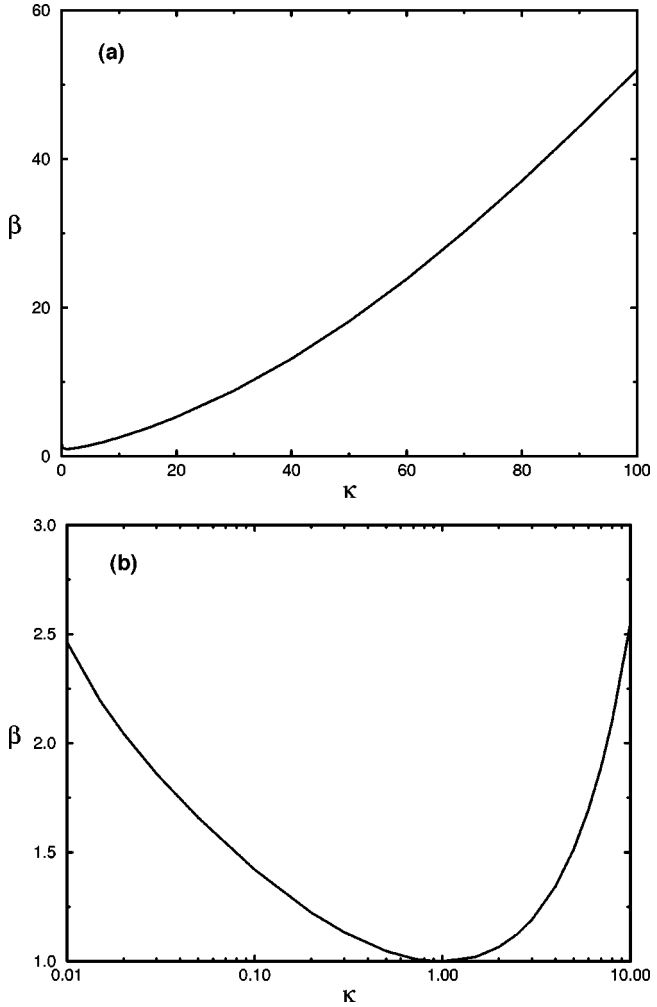

FIG. 7. Plot of β as a function of κ: (a) general view; (b) detail for $\kappa\leqslant 10$.

Figure 8 shows several $F(Q)$ curves for various values of κ. Similar to the case of $\kappa=3$, opportunities for obtaining a repulsive electrostatic force are rather limited (in the interval between the two roots of positive values) in general for two nearby particles of $\kappa>1$, due to the positive dielectrophoretic effect. A significant attractive electrostatic force (positive F) appears either when two particles carry opposite signed charge as described by negative values of Q or when the same-signed charges on two particles differ considerably in amount as represented by large positive values of Q. As κ increases from unity, the two roots converge to $Q=1$ as a consequence of $\beta/\alpha\rightarrow 2$ [cf. Eq. (10)]. Moreover, the magnitude of the repulsive electrostatic force is also limited by a finite extreme value, whereas the magnitude of the attractive electrostatic force has no physical limit. For $\kappa<1$, the situation is just the opposite due to the negative dielectrophoretic effect. Attractive electrostatic force can only be obtained in the interval between the two negative valued roots and its magnitude is limited by the finite extreme value. The common-sense based intuition that particles with like charges repel and those with opposite charges attract can be

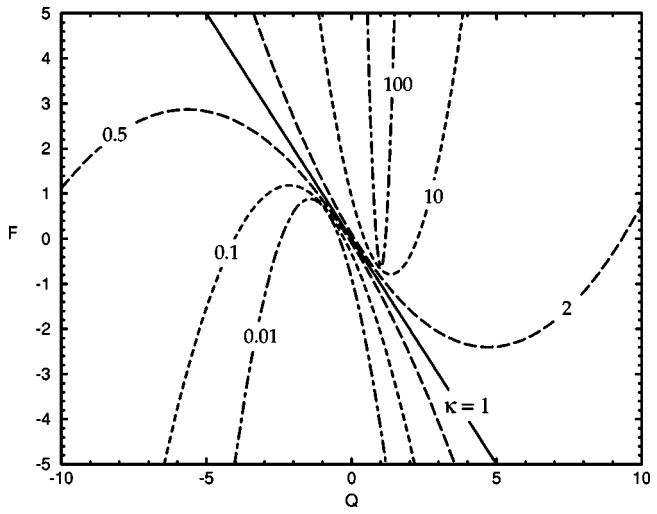

FIG. 8. Curves of F vs Q for $\kappa = 0.01$ (dot-dashed), 0.1 (dashed), 0.5 (long dashed), 1 (solid), 2 (long dashed), 10 (dashed), and 100 (dot-dashed). Bordered by the solid line of $\kappa = 1$, the curves on the left correspond to $\kappa < 1$, whereas those on the right are for $\kappa > 1$. The electrostatic force becomes attractive when $F > 0$ and repulsive when $F < 0$.

strictly applicable only to particles of unity dielectric constant ($\kappa = 1$ as described by a degenerated line in Fig. 8) when dielectrophoretic effects vanish. Therefore, confusing results are expected in the dielectric force measurements with Coulomb's torsion balance (cf. Ref. [8]) when the separation between two spheres becomes relatively small.

For convenience of reference, the difference and median value of the two roots $|\Delta Q|$ and Q_m as well as the value of $F(Q_m)$ are listed in Table I for various κ. The relative range covered between the two roots as represented by $|\Delta Q|$ is shrinking as κ moves away from unity. The two roots as well as Q_m converge to $Q = 1$ and $Q = -1$, with $\kappa \to \infty$ and $\to 0$, respectively. The magnitude of $F(Q_m)$ is always less than that of Q_m, as consistent with the physical expectation that the dielectrophoretic effect reduces the net interaction force at $Q = Q_m$ from that described by Coulomb's law for the force between two point charges located at the centers of the two spheres (as represented by the line in Fig. 8 for $\kappa = 1$).

TABLE I. Values of $|\Delta Q|$, Q_m, and $F(Q_m)$ for various κ.

κ	$\lvert\Delta Q\rvert$	Q_m	$F(Q_m)$
0.001	0.868 78	−1.090 27	0.739 58
0.01	2.023 27	−1.422 47	0.886 28
0.05	3.022 77	−1.812 26	1.045 47
0.1	3.783 06	−2.139 60	1.187 68
0.5	11.130 37	−5.654 32	2.870 33
0.8	32.842 58	−16.451 70	8.241 85
2	9.212 13	4.713 37	−2.399 30
5	3.230 54	1.899 76	−1.038 84
10	1.831 01	1.355 78	−0.786 88
20	1.085 63	1.137 83	−0.686 20
50	0.538 91	1.035 67	−0.632 13
100	0.311 65	1.012 07	−0.623 79
1000	0.099 53	1.001 24	−0.615 36

In spite of the shrinking range between the two roots, the ratio $F(Q_m)/Q_m$ appears to approach nonzero limit values as κ increases or decreases from unity. As $\kappa \to 1$, $F(Q_m)/Q_m$ approaches -0.5 from both sides.

V. CONCLUDING REMARKS

The equation governing the electrostatic interaction between two touching dielectric spheres of equal size and permittivity with each sphere carrying an arbitrary amount of charge is solved here by means of Galerkin finite-element computations. Physically recognizing a quadratic relationship, Eq. (6), enables an efficient means to determine the electrostatic force on each sphere as a function of the net charge ratio of the two spheres $F(Q)$. By virtue of the system symmetry [consequently $\alpha = \gamma$ in $F(Q)$], only two solutions at two different values of the charge ratio Q need to be computed for a given value of the particle dielectric constant κ. For systems without the symmetry, three solutions at three different values of Q should be sufficient for determining the three coefficients α, β, and γ in Eq. (6) at a given κ. Unlike most previous publications on two electrified particles with the limitations either due to the bispherical coordinate system or the simple geometry for image charge expansions, the computational method described in the present work is quite versatile and can be readily extended to a great variety of problem configurations involving many more particles with even irregular particle shapes. Restricting the analysis to the case of two equal-sized spheres here is not due to the limitation of the computational method; it is rather for a better focused analysis that provides important physical insights.

When $\kappa = 1$, polarization effects vanish and the quadratic function of $F(Q)$ degenerates to a linear function because $\alpha = \gamma = 0$ and $\beta = 1$ in Eq. (6). For the case of $\kappa > 1$ where the positive dielectrophoretic effect appears, the two nearby dielectric particles are more susceptible to an attractive electrostatic force even when they carry charges of the same sign. Repulsive electrostatic force can only be obtained in a restrictive range of charge ratio values, which is shrinking with increasing κ. Thus, attractive electrostatic force can occur even when the two spheres carry charges of the same sign. In contrast, negative dielectrophoretic effect comes into play when $\kappa < 1$, such that attractive electrostatic force between two nearby dielectric particles cannot be obtained outside a restrictive range of charge ratio values. Two nearby dielectric particles of $\kappa < 1$ can experience a repulsive electrostatic force even when they carry charges of the opposite sign. In the presence of dielectrophoretic effect, whether the electrostatic force between the two spheres is attractive or repulsive is determined by the ratio of charge on the two spheres.

In a typical powder or granular material, the surrounding medium is air or a gas with permittivity about the value of vacuum and therefore κ is greater than unity. Although the bulk averaged net charge should be zero on a macroscopic scale, each dielectric particle is likely to carry a charge different from its neighbors either in amount or sign due to the stochastic nature of the triboelectric charging process. Hence, electrostatic force among charged dielectric particles is expected to enhance the macroscopic cohesivity of powder

or granular materials, due to the positive dielectrophoretic effect between neighboring particles. For a dense suspension of charged dielectric particles in a dielectric liquid medium where the Debye length is much greater than the particle size, negative dielectrophoretic effect may come into play when the liquid permittivity becomes greater than solid particles (i.e., $\kappa<1$). Negative dielectrophoretic effect can help prevent particles from forming aggregates and therefore stabilize the suspension.

ACKNOWLEDGMENTS

The author would like to thank Dr. Dan Hays for frequent discussions and Dr. Keith Watson for thoughtful suggestions.

[1] The effects of particle charge on granular flow rheology is a largely unexplored area of research. The lack of discussion of these effects in the granular flow literature should not be interpreted as a dismissal of their importance, as commented on by H. Ahn and C. Brennen, in *Particulate Two-Phase Flow*, edited by M. C. Roco (Butterworth-Heinemann, Boston, 1993), p. 210.
[2] W. R. Harper, *Contact and Frictional Electrification* (Oxford University Press, London, 1967).
[3] J. H. Dessauer and H. E. Clark, *Xerography and Related Processes* (The Focal Press, London, 1965).
[4] R. Schaffert, *Electrophotography* (Focal/Hastings House, New York, 1975).
[5] L. B. Schein, *Electrophotgraphy and Development Physics*, 2nd ed. (Laplacian, Morgan Hill, 1996).
[6] M. Poisson, Mem. Sci. Math. de l' Inst. Imp. Fr. **12**, (1811) (as cited by Davis [11]). Poisson's work on two conducting spheres was also mentioned in Maxwell's treatise [8] without clear citation.
[7] W. Thomson, Philos. Mag. **5**, 287 (1853).
[8] J. C. Maxwell, *A Treatise on Electricity and Magnetism* (Oxford University Press, London, 1881).
[9] A. Russell, Proc. R. Soc. London, Ser. A **82**, 524 (1909).
[10] P. M. Morse and H. Feshbach, *Methods of Mathematical Physics* (McGraw-Hill, New York, 1957).
[11] M. H. Davis, Q. J. Mech. Appl. Math. **17**, 499 (1964); also available in a form of RAND Memorandum of January 1964 (RM-3860-PR).
[12] H. B. Levine and D. A. McQuarrie, J. Chem. Phys. **49**, 4181 (1968).
[13] A. Goyette and A. Navon, Phys. Rev. B **13**, 4320 (1976).
[14] J. D. Love, Q. J. Mech. Appl. Math. **28**, 449 (1975).
[15] R. D. Stoy, J. Appl. Phys. **65**, 2611 (1989).
[16] R. D. Stoy, J. Appl. Phys. **66**, 5093 (1989).
[17] P. C. Chaumet and J. P. Dufour, J. Electrost. **43**, 145 (1998).
[18] W. D. Hall and K. V. Beard, Pageoph. **113**, 515 (1975).
[19] S. N. Grover, Pageoph. **114**, 521 (1976).
[20] Y. Nakajima and T. Sato, J. Electrost. **45**, 213 (1999).
[21] D. J. O'Meara, Jr. and D. A. Saville, Q. J. Mech. Appl. Math. **34**, 9 (1981).
[22] R. Becker, *Electromagnetic Fields and Interactions* (Blaisdell, London, 1964).
[23] T. B. Jones, J. Electrost. **18**, 55 (1986).
[24] T. B. Jones, *Electromechanics of Particles* (Cambridge University Press, Cambridge, England, 1995).
[25] W. R. Smythe, *Static and Dynamic Electricity* (McGraw-Hill, New York, 1950).
[26] L. Poladian, Q. J. Mech. Appl. Math. **41**, 395 (1988).
[27] I. V. Lindell, J. C. E. Sten, and K. I. Nikoskinen, Radio Sci. **28**, 319 (1993).
[28] N. S. Goel and P. R. Spencer, in *Adhesion Science and Technology, Polymer Science and Technology*, edited by L.-H. Lee (Plenum, New York, 1975), Vol. 9B, p. 763; Also see more detailed derivations in the work of F. P. Buff and N. S. Goel, J. Chem. Phys. **56**, 2405 (1972).
[29] G. C. Hartmann, J. E. Marks, and C. C. Yang, J. Appl. Phys. **47**, 5409 (1976).
[30] W. Y. Fowlkes and K. S. Robinson, in *Particles on Surfaces: Detaction, Adhesion, and Removal*, edited by K. L. Mittal (Plenum, New York, 1988), p. 143.
[31] D. A. Hays, J. Adhes. Sci. Technol. **9**, 1063 (1995).
[32] G. Strang and G. J. Fix, *An Analysis of the Finite Element Method* (Prentice-Hall, Englewood Cliffs, NJ, 1973)
[33] J. Q. Feng and D. A. Hays, IEEE Trans. Ind. Appl. **34**, 84 (1998).
[34] J. Q. Feng and T. C. Scott, J. Fluid Mech. **311**, 289 (1996).
[35] L. A. Bozzi, J. Q. Feng, T. C. Scott, and A. J. Pearlstein, J. Fluid Mech. **336**, 1 (1997).
[36] T. J. R. Hughes, *The Finite Element Method, Linear Static and Dynamic Finite Element Analysis* (Prentice-Hall, Englewood Cliffs, NJ, 1987).
[37] J. Q. Feng, J. Comput. Phys. **151**, 969 (1999).
[38] J. M. Ortega and W. C. Rheinboldt, *Iterative Solution of Nonlinear Equations in Several Variables* (Academic, London, 1970).